Biosensors and Bioelectronics 145 (2019) 111701

Contents lists available at ScienceDirect

Biosensors and Bioelectronics

journal homepage: www.elsevier.com/locate/bios

Platelet-driven formation of interface peptide nano-network biosensor enabling a non-invasive means for early detection of Alzheimer's disease

Kai Zhang[a,**,1], Qianlu Yang[c,1], Zhenqiang Fan[a,d], Jianfeng Zhao[d], Hao Li[b,*]

[a] Key Laboratory of Nuclear Medicine, Ministry of Health, Jiangsu Key Laboratory of Molecular Nuclear Medicine, Jiangsu Institute of Nuclear Medicine, Wuxi, Jiangsu, 214063, China
[b] School of Biological Science and Technology, University of Jinan, No. 106 Jiwei Road, Jinan, Shandong, 250022, China
[c] Department of Biochemistry and Molecular Biology, Nanjing Medical University, Nanjing, 211166, Jiangsu, China
[d] Key Laboratory of Flexible Electronics (KLOFE) & Institute of Advanced Materials (IAM), Jiangsu National Synergetic Innovation Center for Advanced Materials (SICAM), Nanjing Tech University (NanjingTech), 30 South Puzhu Road, Nanjing, 211816, PR China

ARTICLE INFO

Keywords:
Platelet-driven
Nano-network biosensor
Alzheimer's disease

ABSTRACT

Soft material fabricated with DNA origami or peptide cross-linking technique may be promising theranostic platforms in the future; however, their naturally occurring counterparts, such as the peptide aggregates in the neurodegenerative diseases, constitute an increasingly burdensome issue of public health. Thus, a design of artificial peptide nano-network biosensor is conceived, in an attempt to combat the natural pathological peptides, by mimicking their pathogenesis process. Specifically, periphery platelet can secrete A-beta and induce its cross-linking & aggregation to form a surface peptide nano-network, resulting in large numbers of poly-tyrosine strands being covalently trapped in the network to serve as an efficient signal amplifier, through the electrochemical oxidation of tyrosine. This method is sensitive and quantitative in the range of normal and pathological periphery platelet distribution and can effectively discriminate Alzheimer's disease (AD) patients based on the detected potential neurodegenerative activity of platelet. These results may point to some future perspective of this method in the early screening of AD.

1. Introduction

Soft matter such as biomaterial fabricated via DNA origami or amino acid cross-coupling enable bio-compatible theranostic platforms for targeted and smart drug delivery, biosensing, establishing artificial cell-cell contact, etc. On the other hand, such high order nano-assembly also occurs in the cellular life, sometimes in a menacing manner as in the neurodegenerative diseases. The social and economic burden of neurodegenerative diseases such as Alzheimer's disease (AD) are more and more keenly felt by many a country experiencing population ageing (Iqbal et al., 2016; Przedborski, 2017; Saudou and Humbert, 2016; Singleton and Hardy, 2016). Although these diseases are currently without effective treatment, the early diagnosis of these conditions may still help to alleviate the accompanied social burden. Traditionally, diagnosis is based on symptoms such as memory loss and dementia, and confirmed by autopsy of patients' brain to spot the amyloid-like plaques (Hughes et al., 2017; Mortamais et al., 2017; Takahashi et al., 2017). Less invasive methods are gradually established, for example, elevated amyloid beta (A beta) in the cerebrospinal fluid (CSF) is a reliable marker of AD; but the collection of CSF still requires lumbar puncture, often a painful experience on the part of the patients (Toledo et al., 2013). Reliable non-invasive detection of the amyloid plaque in brain has recently been established using positron emission tomography (PET) to track injected labels that can bind with aggregates of A beta with high affinity (Toledo et al., 2013). Although non-invasive, this method also requires exposing the patients to radiation strong enough to ionize the injected label for signal readout, besides the high cost of the instruments (Toledo et al., 2013). Moreover, apart from this difficulty in achieving low-cost and non-invasive detection, there is a more fundamental issue concerning the amyloid plaques or aggregates, namely the major target in the above detection methods: these aggregations may rather be the end product of AD development, than the previously supposed major source of AD-associated neurotoxicity (Ferreira et al., 2015; Schuster and Funke, 2016; Sengupta et al., 2016; Smith and Strittmatter, 2017; Viola and Klein, 2015). For AD often has a prolonged preclinical phase lasting, in some cases, for two to three

* Corresponding author.
** Corresponding author.
E-mail addresses: zhangkai@jsinm.org (K. Zhang), cardely@126.com (H. Li).
[1] Both authors contributed equally to this work.

https://doi.org/10.1016/j.bios.2019.111701
Received 30 August 2019; Received in revised form 11 September 2019; Accepted 12 September 2019
Available online 13 September 2019
0956-5663/

decades, during which process misfolded A beta already exists in the forms of soluble monomer, dimer and oligomers (Ferreira et al., 2015; Schuster and Funke, 2016; Sengupta et al., 2016; Smith and Strittmatter, 2017; Viola and Klein, 2015). Under inflammatory conditions such as oxidative stress, such soluble A beta can combine with metal ion and other bioactive cofactors to engage in a self-amplifying and vicious circle of neurodegenerative oxidative damage (Li et al., 2016). It is such mechanism, in force early on, that promotes the AD development, into amyloid plaques with memory loss and dementia as the symptoms, marking a somewhat advanced and uncontrollable stage of AD. Therefore, a non-invasive method that can detect such early activity of A beta may be greatly welcomed as a new means for AD risk evaluation and early screen.

Interestingly, assaying the activity of such soluble A beta (Janelidze et al., 2016; Pérez-Grijalba et al., 2013; Rissman et al., 2012; Ruiz et al., 2013; Song et al., 2011) may actually open up new opportunity for cost-effective and non-invasive means of detecting AD. Although the cytotoxic activity of such soluble A beta is dominantly observed in the central nervous system, evidences, although sporadic and isolated, also indicate similar activities observed in the platelets (Catricala et al., 2012; Chen et al., 1995). In fact, platelet, possessing the full range of A beta-processing enzymes of the central nervous system, may be viewed as a periphery model of AD, mirroring that condition in all the steps of its development (Gowert et al., 2014). Platelet can be readily collected via peripheral blood sampling, which is conventionally considered non-invasive; meanwhile, platelet is in fact downsized and anucleated cell, proven to be easier to analyze than the neurons. When platelet is activated to process and release A beta (Casoli et al., 2010; Smirnov et al., 2009), the accompanying oxidative stress results in self-catalyzed cross-linking. This self-propagated A beta assembly and covalent coupling to form two-dimensional peptide network can be employed to mimic the neurotoxic activity of A beta. This activity-driven formation of peptide network provides a nano-sensing surface for effective signal amplification.

Here, this design rationale is employed, and a bioassay is designed to evaluate the neurodegenerative capability of platelet-secreted A beta in forming and catalyzing oxidative cross-linking. Biosensing surface modified by peptide-based probes, containing both A beta-targeting sequence (Lowe et al., 2001) and the A beta 25～35 fragmented sequence (Scheme 1a), is brought to interact with platelet fractioned from blood sample (Scheme 1b). The A beta 25～35 sequence, upon contact with platelets, can activate them to secrete A beta (Scheme 1c), and can also elevate ROS (reactive oxygen species) production and other cytotoxic reactions (Canobbio et al., 2014; Shen et al., 2008). The platelet-secreted A beta can then be captured by the targeting sequence on the peptide probes (Lowe et al., 2001) (Scheme 1c). Both A beta and the activated platelet can employ the ROS generated to modify themselves, to cross-link and to aggregate (Gowert et al., 2014), paralleling the neurodegenerative process of A beta fertilization and aggregation. To characterize this process, poly-tyrosine (40～200) is added to the biosensing system (Scheme 1d), as a co-substrate of the oxidative modification and cross-linking. So that platelets of higher neurodegenerative potential may result in more extensive cross-linking and immobilization of poly-tyrosine (as well as platelet-secreted A beta) onto the surface-tethered peptide (Scheme 1e), through the same di-tyrosine cross-coupling mechanism as observed in A beta (Al-Hilaly et al., 2013) and many other proteins (Alhilaly et al., 2016; Diehl and Brown, 2014; Faccio et al., 2014; Minamihata et al., 2011). The covalent linkage so formed then allows thorough and violent rinsing to be applied to remove absorbed interfering species. This surface peptide network can then yield amplified signal readout through electrochemical oxidation and decomposition of the large numbers of tyrosine moieties (Gao and Cranston, 2010). It is also worth noting that the sequence of the designed biosensor (Fig. S1), also contains a single tyrosine residual as anchor points of the cross-linked product. And the surface density of these probes can be regulated to a relatively low level, so as to prevent the direct cross-linking between them, as will be described below.

The blood sampling and platelet fractionation are simple, well-established and everyday clinical practice, while the proposed method only involves one-step incubation and reaction before the collection of signal readout. Using this simple protocol, blood samples from AD patients and healthy volunteers are compared and the detected sensing signal may to some extent parallel the progress of AD. This method may hold the promise to be further validated in progressive studies on AD development in the future, and may one day afford a new means for AD preclinical detection and risk evaluation.

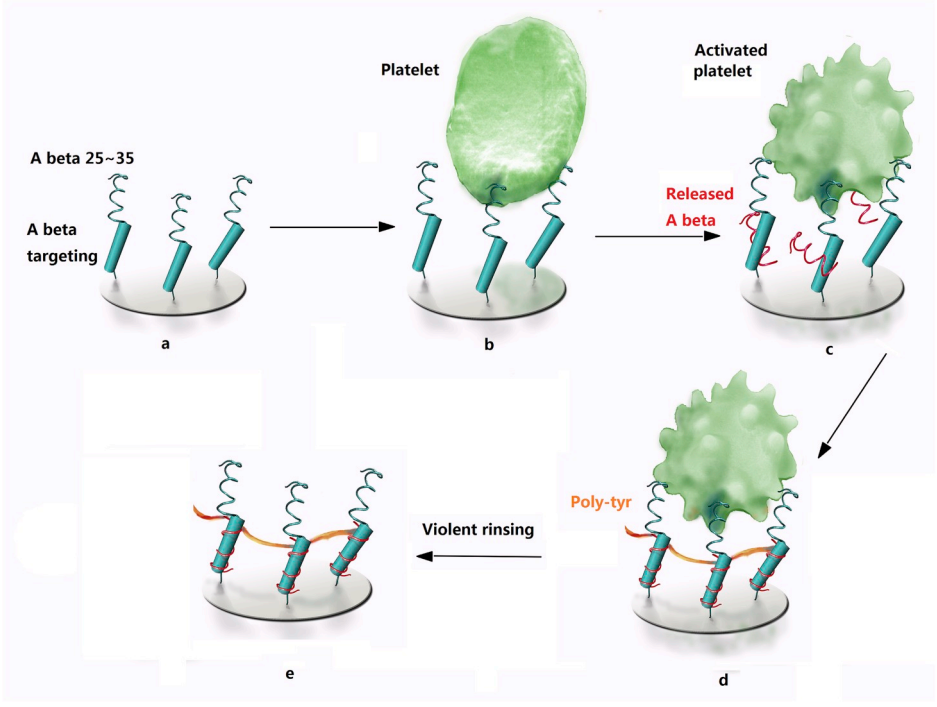

Scheme 1. The proposed method using platelet-driven formation of peptide network to evaluate the degenerative activity of A beta. For clearance, poly-tyr is shown added after platelet incubation, but the standard procedure proposed here is to mix this co-substrate with the platelet sample before incubation with the ITO slide. Not drawn to scale.

2. Experimental

2.1. Chemicals and biological materials

Peptide probe (11-Mercaptoundecanoic acid (MUA)-KLVFFEEEEEE -Y-GSNKGAIIGLM) was custom-synthesized as lyophilized powder, purity > 95%, by Congbeibio Co, Ltd. Poly-tyrosine (10,000 –40,000 Da, around 50–200 tyrosyl moieties) and thioflavin-T were purchased from Sigma-Aldrich. Platelet samples employed as the analyte were sampled from healthy volunteers, for the design validation and optimization of experimental conditions, and from patients for clinical sample detection, following the standard protocol: 5 mL blood was vein-sampled into the yellow cap tube containing 39 mM citric acid, 75 mM sodium citrate, and 135 mM glucose, pH 7.4; followed immediately by 190 g centrifugation at room temperature for around 15 min, the upper fraction (roughly 2 ml) was rich of platelet. This upper fraction was collected, counted and centrifugated at 2500 g at room temperature for 5 min, finally resuspended with 10 mM phosphate buffered saline (PBS) (pH 7.4). For detection, the platelets were short-termed cultured in 24 well culture plates at a density of 1×10^6 cells/cm^2, co-incubated with thrombin for gradually longer time at 37 °C. All the other chemicals were of analytical-grade. The solutions of the peptide biosensor were prepared by dissolving the powder to 10 μM with 10 mM phosphate buffer solution (PBS) (pH 7.4), poly-tyrosine was dissolved with the same solution to a nominal concentration of 200 μM using 25,000 Da to represent the molecular weight. All solutions were prepared with double-distilled water, which was purified with a Milli-Q purification system to a specific resistance of 18 MΩ•cm. MDA-MB-231 (ATCC) was maintained in Leibovitz's L-15, 10% fetal bovine serum, and in a humidified atmosphere with no extra CO_2 at 37 °C. MCF-7, HEK293T were received as a gift from Prof. Jiadong Huang of the School of Life Sciences of the University of Jinan. For detection, the cells were seeded in 24 well culture plates at a density of 1×10^4 cells/cm^2. The cells were then collected, diluted (each sample contains roughly 1×10^5 cells) and fractioned using a nuclear extraction kit. The cytoplasmic samples were then used for detection. For the detection of clinical samples, serum samples were collected from AD patients at Shandong Tumor Hospital after elected consent by the local ethical committee; platelet was fractioned according to the above description.

2.2. Electrode treatment

Transparent Au slides (ITO slides ion-sprit with roughly 100 Å Au layer) were cut to fit the size of the cuvette used for fluorescence measurement. These slides were cleaned by ethanol sonication for 5 min, and dried under a mild stream of high purity nitrogen, followed by immerging in the assembly solution (5 μM probe 5 mM Tris (2-carboxyethyl)phosphine hydrochloride (TCEP) in 10 mM PBS, pH 7.4) at 4 °C for 16 h, TCEP was to prevent disulphide between probes. The slides were then immerged in 9-mercaptononanol (MN) solution (1 mM MN in 10 mM PBS, pH 7.4) at room temperature for 3 h.

2.3. Detection

Fractioned and diluted platelet was mixed with 200 μM poly-tyrosine at a 1:1 ratio and was incubated with the slide for 1 h at 37 °C, the slides were then thoroughly rinsed with Sodium dodecyl sulfate (SDS) for electrochemical measurements.

2.4. Experimental measurements

Isothermal titration calorimetry (ITC) measurements were conducted using a MicroCal ITC200 System (GE healthcare life sciences). The titration was conducted at 25 °C. The titration schedule consisted of 38 consecutive injections of 1 μL with at least a 120 s interval between injections. Heats of dilution, measured by titrating beyond saturation, were subtracted from each data set. All solutions were degassed prior to titration. The data were analyzed using Origin 7.0 software. Fluorescence emission spectra of surfaces were measured using a QM-4/2005 fluorescence spectrometer (Photon Technology International, Inc., Birmingham, NJ) equipped with a xenon lamp. This light source and the detector were in the same plane at right angle to each other. The slides were kept in a water-filled cuvette at 60° from the base of the cuvette for fluorescence measurements. The surface with gold film was kept away from the light source and towards the detector. Activating peak wavelength for dityrosine is 325 nm, while that for 3,4-Dihydroxyphenylalanine (DOPA) is around 360 nm. Surface plasma resonance (SPR) measurements were performed with an Autolab ESPRIT system (Echo Chemie B.V., Netherlands) equipped with a 670 nm monochromatic p-polarized light resource. Electrochemical measurements were carried out on a CHI660D Potentiostat (CH Instruments) with a conventional three-electrode system: the modified electrode as the working electrode, a saturated calomel electrode (SCE) as the reference electrode and a platinum wire as the counter electrode. Square wave voltammograms (SWVs) were recorded in 10 mM PBS, pH 7.4, which was deoxygenated by purging with nitrogen gas and maintained under this inert atmosphere during the electrochemical measurements. The experimental parameters for EIS: bias potential, 0.224 V vs. SCE; amplitude, 5 mV; frequency range, 0.1 Hz ~ 10 kHz electrolyte solution: 5 mM $Fe(CN)_6^{3-/4-}$ with 1 M KCl. The data are obtained from at least three times of repetition of independent experiment, error bars are shown in the figures. Circular dichroism (CD) spectra were obtained using a JASCO J-750 circular dichroism spectrometer, at wavelength and scan speed of 190–260 nm and 500nm/min, respectively. Fourier transform infrared (FT-IR) spectroscopy was conducted and the FT-IR spectra were obtained on a Nicolet iS10 (Thermo Nicolet, America). The spectra were recorded at room temperature in transmission mode. Dynamic light scattering (DLS) measurements were conducted on a particle size analyzer (Brookhaven 90Plus, USA) under the batch mode (scattering angle, 15°) and at 25 °C.

3. Results and discussion

3.1. The working principle

The proposed method, as illustrated in Scheme 1 and described above, is first validated using electrochemical impedance spectroscopy (EIS) (Fig. 1ã c), since drastic change of surface resistance can be induced during the proposed detection procedure, and this may be most conveniently characterized by this method. The sensing surface is incubated with platelet sample (mixed with the poly-tyrosine co-substrate), or with poly-tyrosine alone; following the standard sensing procedure as depicted in Scheme 1. The resulted EIS are compared (Fig. 1a), the spectrum in the absence of platelet (curve B) shows a resistance insignificant compared with that obtained after surface cross-linking after incubation with target platelet (curve A), indicating no retention of poly-tyrosine on the sensing surface without platelet secretion of A beta and subsequent peroxidase-like activity. On the contrary, following violent detergent rinsing step, the residual impedance of the experimental group (curve A) is still evidently larger than the control, indicating covalent retention of platelet-secreted A beta and the poly-tyrosine co-substrate. The incubation with platelet & poly-tyr mixture is stopped after gradually longer time of incubation. Without rinsing, the surface is immediately brought to EIS measurement. The resulted spectra (Fig. 1b) show only moderately evident difference with respect to incubation time; all the recorded impedance seem to indicate large amount of platelet in contact with the surface. In contrast, if the same steps are repeated, but with violent rinsing before each EIS measurement, the results show a gradual increase with incubation time (Fig. 1c), indicating gradual accumulation of covalently retained species. These results are mirrored by the SPR sensorgrams (Fig. 1d1 ~ 3),

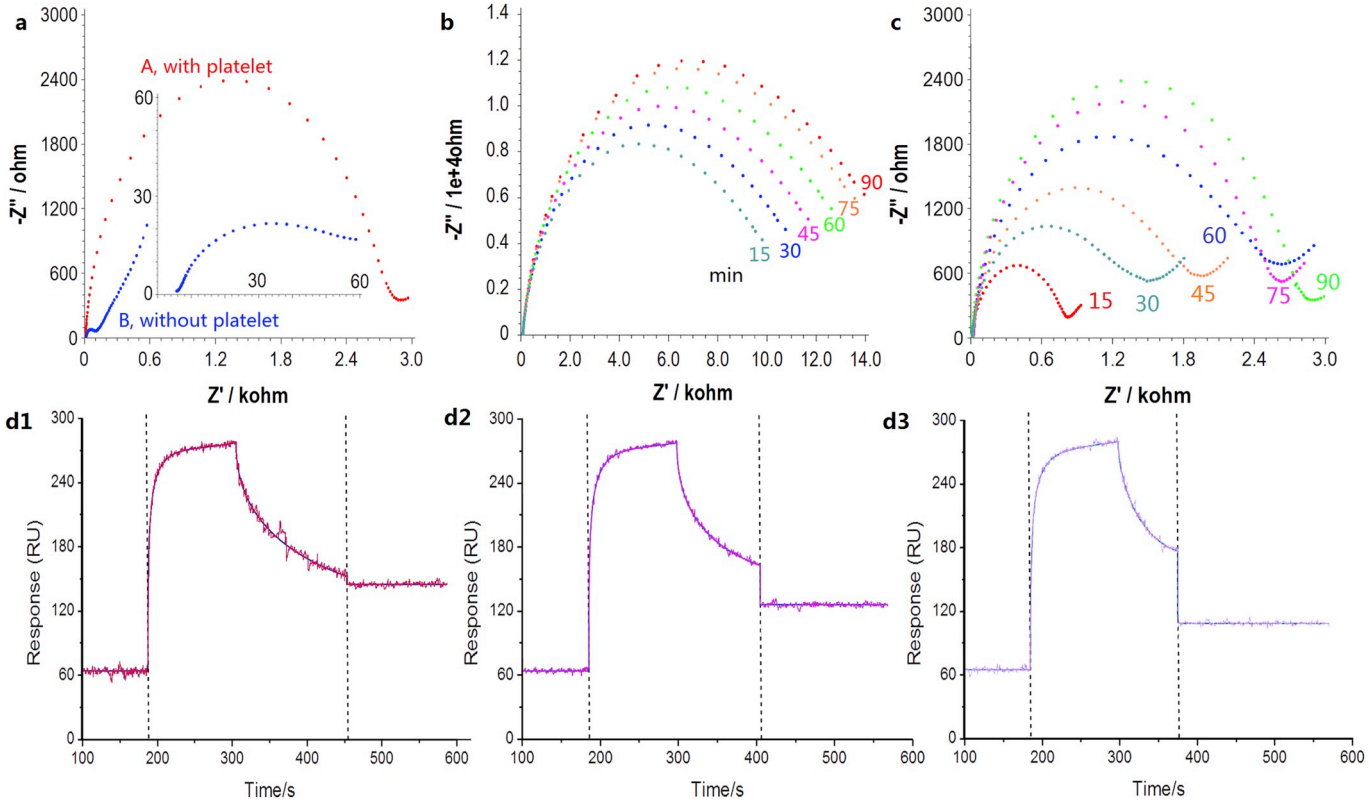

Figure 1. (a)~(c) Electrochemical impedance spectra (EIS) recorded on the peptide based biosensor modified electrode under various conditions: (a) incubation with 100 × 10^6/mL platelet, with the incubation in the blank buffer as a control, inset of panel a shows the initial part of the blue Curve A, unit of both axis is ohm. (b) incubation with the same target for gradually longer time, without further rinsing before EIS recording, (c) after the same operation as in (b), followed by thorough detergent rinsing. (d) SPR sensorgrams obtained by flowing platelet (the above concentration) across a sensing surface modified by the peptide probe, from d3 to d1, the addition of detergent starts gradually later.

in which, the same accumulation time of platelet results in almost the same "on-off" time curve, while gradually longer incubation before violent rinsing results in larger retention (from d3 to d1). Together, these results confirm that only after the activity of platelet can poly-tyr, and perhaps also amyloid-beta secreted by platelet, be covalently retained.

3.2. Optimization of experimental conditions

Key steps of the sensing procedure are particularly investigated to further consolidate the above results. After incubation with platelet (without poly-tyr), the surface is subject to gentle detergent rinsing using 5% tween-20. The possible presence of surface captured A beta secreted by the platelet is examined using thioflavin-T, a dye targeting A beta (Xue et al., 2017). Although the gentle rinsing, by removing the platelet, may at the same time also remove some of the surface captured A beta, the electrochemical response of thioflavin-T can still be evidently observed (Fig. 2a), increasing with platelet concentration, indicating capture of platelet secreted A beta while the ability of the biosensor and thioflavin-T to specifically bind with A beta is also confirmed using isothermal calorimetry (ITC) (Fig. 2b, left and right, respectively). Following the standard procedure in Scheme 1, in the finally resulted surface product, fluorescence of di-tyrosine is present (Fig. 2c), in parallel with platelet concentration used, confirming the existence of covalently cross-linked product, the di-tyrosine linkage (Andreev et al., 2002; Mahmoud and Bialkowski, 1995) between the tyrosine containing A beta and poly-tyr. To further specify this, after incubating with platelet but without poly-tyr, tandem tween-20 mild rinsing, some cross-coupling can be observed (Fig. 2d, curve A), indicating platelet catalyzed and perhaps A beta self-catalyzed A beta cross-linking. After further incubation with gradually more concentrated poly-tyr in the presence of H_2O_2, evident cross-linking can be observed (Fig. 2d, curve B~F), suggesting a possible major contribution of A beta catalysis to the above observed cross-linking during the incubation with the platelet & mixture. Taken together, these results also confirm that both the platelet –secreted A beta and the platelets themselves are responsible for surface covalent cross-linking of A beta and poly-tyr.

By electrochemical oxidation, the tyrosine moieties of the surface cross-linked poly-tyr can generate large electrochemical peak response (Fig. 3). As a control, the single tyrosine residual in the biosensor peptide can also generate a small background of tyrosine oxidation (Fig. S3). Formation of the poly-tyr network and the destruction by electrochemical oxidation are examined using various methods (Fig. 4). Destruction of the peptide network after tyrosine electro-oxidation is morphologically evident on AFM graphs (Fig. 4a, Fig. S2). Surface density of the probe has also been investigated, as shown in Fig. S5, which shows an average distance around several hundreds of nanometers separating two surface-immobilized probes, so the possibility of direct cross-linking between probes can be eliminated. To further characterize the poly-tyr network, it is electrochemically "peeled" off the sensing interface using potential scanning over proper range (Widrig et al., 1991), only the "anchoring points" of Au–S bonds on the peptide probes are selectively open up. The collected suspension is studied using DLS, CD and FT-IR spectroscopy (Fig. 4b~d). The DLS data shows evident decrease of the mean size of individual network patches as well as wider size distribution after electrochemical oxidation (Fig. 4d). CD spectrum of the network before electrochemical digestion shows predominant beta-sheet structure that can be attributed to both poly-tyr and A beta (positive peak at 195 nm with much weaker 216 nm negative peak)(Greenfield, 2006), while free coil (negative peaking at 200 nm)(Greenfield, 2006) rises to much more evident after

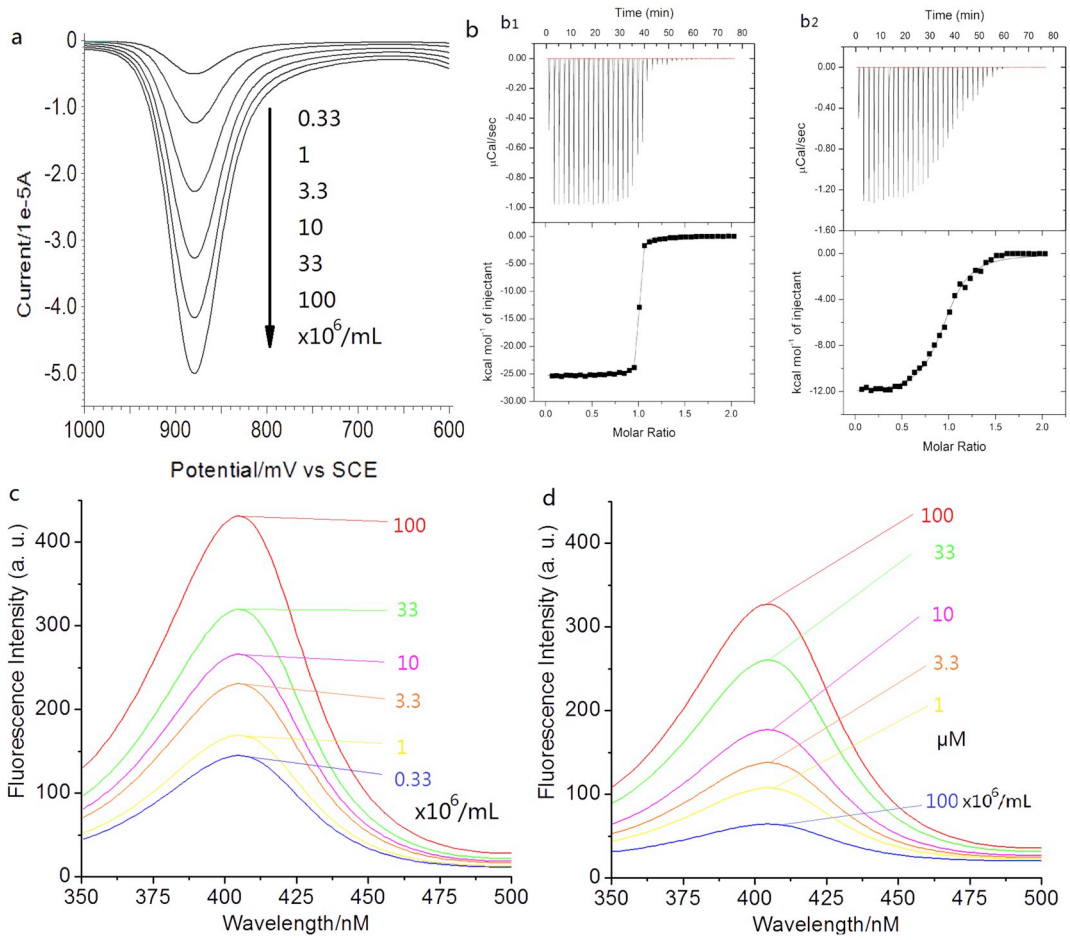

Fig. 2. (a) Electrochemical peak responses of Thioflavin-T characterizing A-beta captured after incubation with gradually higher concentrations of platelet. Panel (b) shows the results of Isothermal titration calorimetry (ITC) titration of 0.5 mM peptide probe into 0.05 mM A beta (left, sub-panel b1) and of 1 mM thioflavin-T into 0.1 mM A beta (right, sub-panel b2) The solution adopted is 10 mM PBS, pH 7.4. The top row displays the raw data of power versus time. The bottom row is the corresponding data by integrating enthalpy values versus the molar ratio of titrant: titrand. These data are fit using Origin 7.0 software, the resulted fitting curve is also shown in the lower row. (c) Fluorescent responses of dityrosine detected after the same treatments in (a). (d) Similar dityrosine responses obtained under control conditions: at the bottom is after incubation with platelet but without poly-tyr co-substrate, the rest is obtained after further incubation with gradually higher amount of poly-tyr as listed on the graph.

the digestion (Fig. 4b), indicating lost of the repeating poly tyr pattern after digestion and the accompanied lost of hydrogen bonding between residuals. On the FT-IR spectra (Fig. 4c), the network peptide before cleavage shows evident amide A peak around 3000 cm^{-1}, associated with extensive hydrogen bonding (Wang et al., 2008); the amide I peak locating at around 1630 cm^{-1} coincides with the CD result, confirming dominant presence of beta sheet structure (Wang et al., 2008); the peak near 1518 cm^{-1} is corresponding to ring-OH(Rosu et al., 2016); while a small peak at 1075 cm^{-1} (di-tyrosyl) suggests relatively low level of cross-linking (Rosu et al., 2016). After digestion, the amide A peak near 3000 cm^{-1} dropped evidently, together with evident dropping of amide I and the enhancing of Amide II around 1510 cm^{-1}, associated with free coil (Wang et al., 2008), these results may suggest a conformational change into this type of unordered existence. The original ring-OH also decreases dramatically with corresponding evident increase around 1075 cm^{-1}, confirming the oxidation of poly-tyr. Together, these results confirm the above electrochemical evidences on the supposed mechanism of peptide network formation, and also the digestion. The stability of the assay has also been studied: peptide probe modified electrode has been kept at 4°C for different time before brought to biosensing steps, and the resulted signal readouts are compared, as summarized in Table S1, which shows satisfactory stability.

3.3. Assay performance

The quantitative performance is first examined using both serially diluted platelet mixture samples and platelet samples subject to gradually longer time of pre-activation[24]. The results (Fig. 3a and b) show signal responses growing in parallel with the platelet concentration or activation time. Linear ranges can be established, with the standard deviation of all repetitive measurements less than 5%. The quantity directly assayed by the proposed method is the number of Abeta-secreting platelet, to relate this quantity to the usually quoted Abeta concentration, we have employed a standard ELISA assay for human Abeta provided by invitrogen to calibrate our assay: the supernate containing secreted Abeta has been separated and the Abeta content has subsequently been quantified by the standard assay. It can be observed that the two mostly diluted samples in Fig. 3a show almost the same ELISA response, the two mostly concentrated samples show a similar trend, this suggests our method has both a larger dynamic range and a lower limit of detection when compared with the standard assay. This result is summarized in Table 1, with the performance of our assay converted into equivalent Abeta concentration (pg/mL), as calibrated by the standard assay.

Similar di-tyrosine cross-linking has been observed and associated with cellular apoptosis process, so possible interference from these sources has also been considered (Fig. 3c and d). Immortalized normal

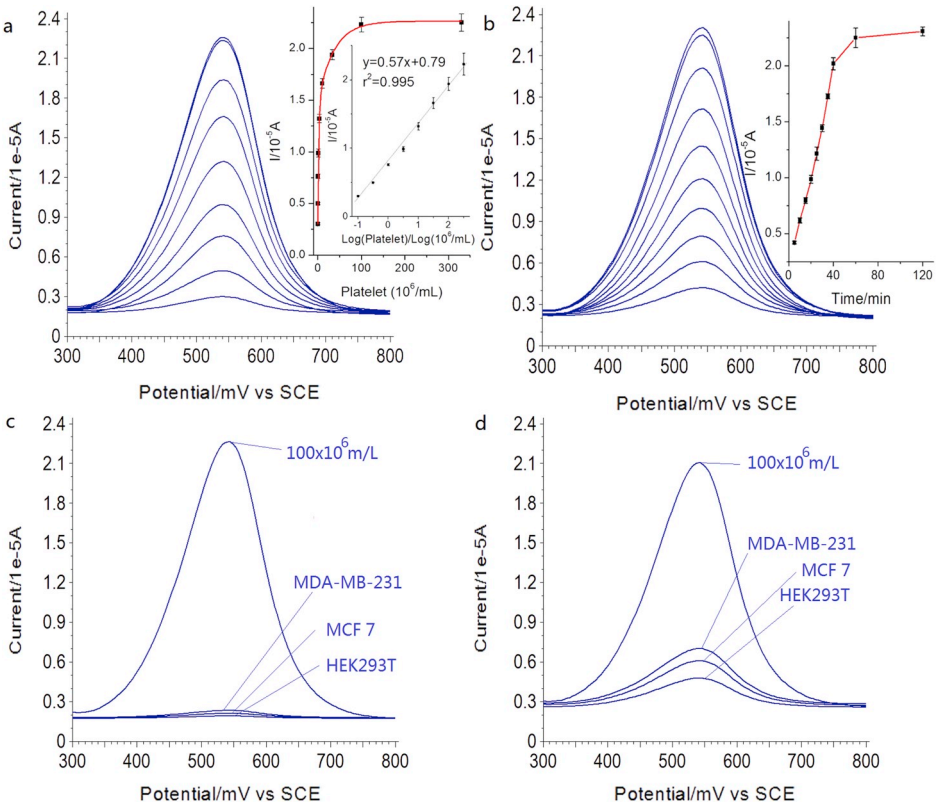

Fig. 3. Analytical performance of the proposed method in the (a) quantitative detection of serially diluted platelet, and (b) 10 × 10^6/mL platelet pre-activated for gradually longer time. The error bars indicate standard deviation (n = 3). (c) Specificity represented by incubation with various cell lines as the control, and (d) incubation with the same set of cell lines directed to apoptosis, as a control.

cell such as HEK 293T can have no platelet-like activity on the sensing surface, while cancer cell such as MCF7 can induce very low-level cross-linking of poly-tyr. Indeed, more malignant cancer cell such as MDA-MB-231 can have more evident effect (Fig. 3c). But all these effects seem negligible compared with that induced by platelet activity. If apoptosis are induced in these cells, the cross-linking effect becomes more evident (Fig. 3d), to some extent comparable with that of the platelet. This is not surprising, since the platelet, after activation,

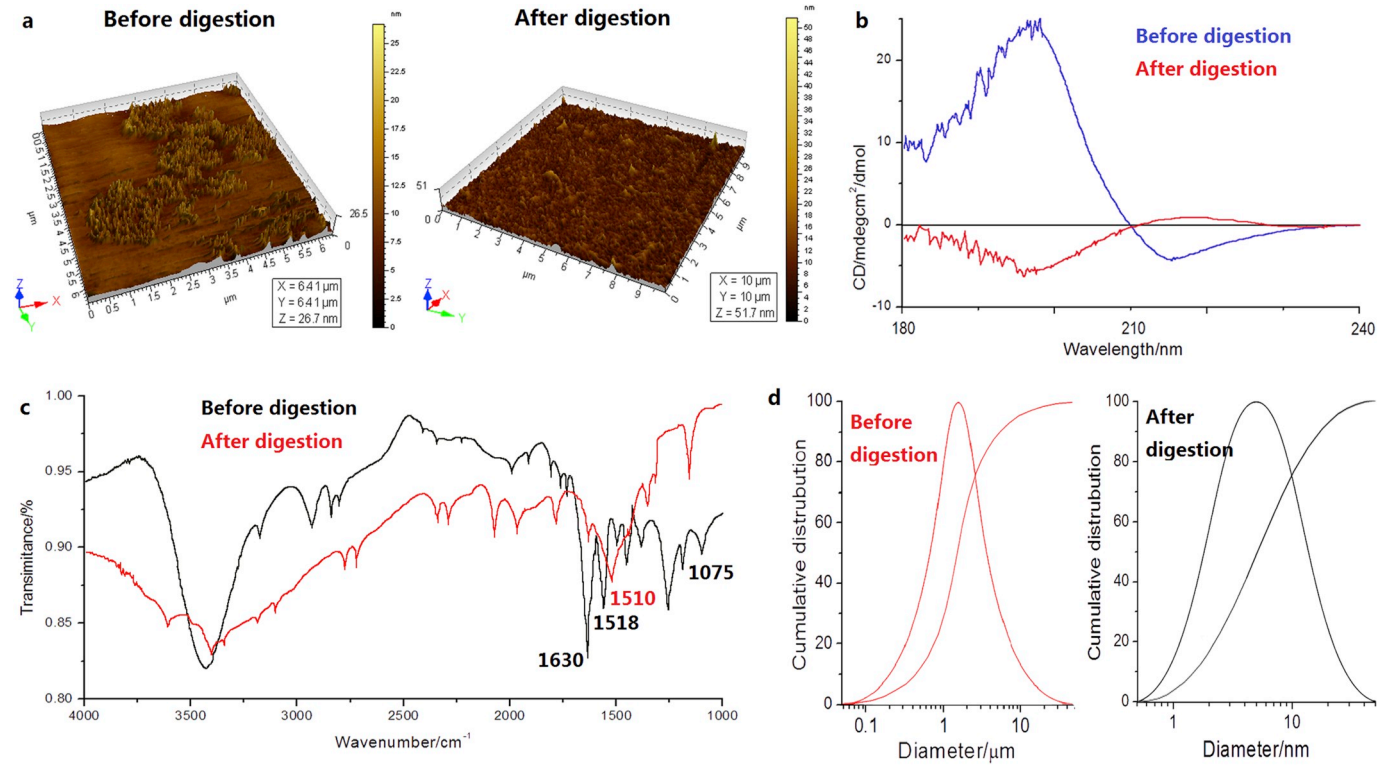

Fig. 4. The peptide network before and after digestion characterized by various methods: (a). Surface morphology examined by AFM (b). Peptide conformation represented by CD spectra. (c) FT-IR and (d) DLS.

Table 1

Method	Dynamic range	Limit of Detection	Standard deviation
ELISA	15.6 ~ 1000 pg/ml	< 10 pg/m	< 5%
This method	3.3 ~ 3300 pg/ml	< 1 pg/ml	< 5%

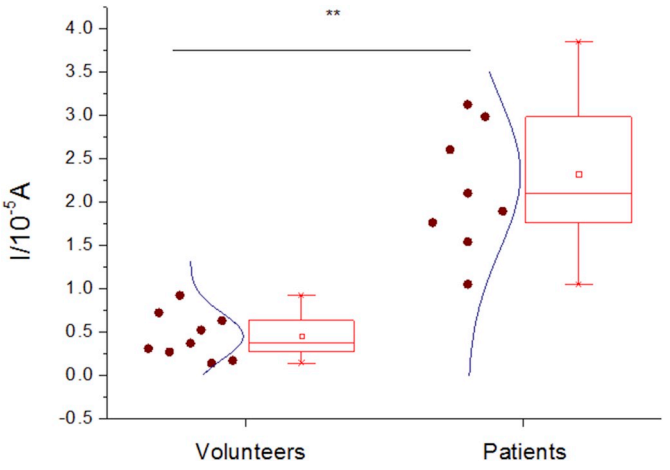

Fig. 5. Box charts showing the distribution of the signal responses in fractioned platelet from healthy volunteers and AD patients. The raw data is included as a column scatter plot to the left of each box. A curve corresponding to normal distribution is also displayed on top of the scatter plot.

undergoes similar apoptotic process; the membrane becomes leaking, while oxidative stress accompanying the process promotes the cross-linking. Since in the blood the platelet is separated with such oxidatively stressed tumor cells in the primary tumor sites, the above results in Fig. 3d may not constitute a major source of interference. These analytical performances are obtained under optimized experimental conditions. The incubation time for the platelet with the electrode is optimized (Fig. S4a), showing 60 min as an optimal time for the interaction between the platelet sample and the surface probe, noting that this reaction is subsequent to and independent of the pre-activation of platelet shown in Fig. 3b, cases of incubation both shorter and longer than this result in reduced signal response. The concentration of poly-tyr is found to be optimal around 100 μM (Fig. S4b), due to signal lose induced by excessive cross-linking.

3.4. Clinical samples assay

To examine the performance in analyzing clinical sample, the blood sample from AD patients and healthy volunteers are collected and fractioned, the platelet fraction is finally reconstituted to the same count per ml, and the signal response is finally compared between the disease and the control groups (Fig. 5). The difference is statistically relevant to the grouping, suggesting possible link between periphery A beta activity with AD, consistent with previous reports and postulations (Catricala et al., 2012; Chen et al., 1995) of using periphery A beta as a marker for the development of AD.

4. Conclusion

In this work, we have established a new method for the early screening of possible development of Alzheimer's Disease based on the detection of A beta in the circulating blood sample. Specifically, platelet from the periphery blood sample is collected and activated, then the platelet belonging to potential AD victim will release amyloid beta that can trigger peptide cross-linking on a peptide probe modified biosensing surface. The cross-linked peptide network can then give rise to amplified electrochemical signal response, enabling sensitive detection of clinical blood samples. Compared with assays using ELISA, our strategy has both a larger dynamic range and a lower limit of detection. Additionally, our nano-network biosensor utilizes poly-tyrosine strands being covalently trapped in the network to serve as an efficient signal amplifier, which provides notable advantages compared to the "label-free" methods. We anticipate that our novel nano-network biosensor could potentially be utilized as an effective biochemical or biomedical technique for AD early screening after improving its stability and repeatability.

CRediT authorship contribution statement

Kai Zhang: Conceptualization, Writing - review & editing, Supervision. **Qianlu Yang:** Data curation, Software, Validation. **Zhenqiang Fan:** Data curation, Software, Validation. **Jianfeng Zhao:** Visualization. **Hao Li:** Supervision, Conceptualization.

Declaration of competing interest

The authors declare that they have no known competing financial interests or personal relationships that could have appeared to influence the work reported in this paper.

Acknowledgment

This work was supported by the National Natural Science Foundation of China (21705061, 810602737, 31700716), the Jiangsu Provincial Key Medical Discipline (Laboratory) (ZDXKA2016017) and the Innovation Capacity Development Plan of Jiangsu Province (BM2018023).

Appendix A. Supplementary data

Supplementary data to this article can be found online at https://doi.org/10.1016/j.bios.2019.111701.

References

Al-Hilaly, Y.K., Williams, T.L., Stewart-Parker, M., Ford, L., Skaria, E., Cole, M., Bucher, W.G., Morris, K.L., Sada, A.A., Thorpe, J.R., 2013. A central role for dityrosine crosslinking of Amyloid-β in Alzheimer's disease. Acta Neuropathol. Commun. 1 (1), 1–17.

Alhilaly, Y.K., Biasetti, L., Blakeman, B.J., Pollack, S.J., Zibaee, S., Abdulsada, A., Thorpe, J.R., Xue, W.F., Serpell, L.C., 2016. The involvement of dityrosine crosslinking in α-synuclein assembly and deposition in Lewy Bodies in Parkinson's disease. Sci. Rep. 6.

Andreev, O.A., Reshetnyak, Y.K., Goldfarb, R.H., 2002. Evidence of inter- and intra-molecular crosslinking of tyrosine residues of calmodulin induced by photo-activation of ruthenium(II). Photochem. Photobiol. Sci. Off. J. Eur. Photochem. Assoc. Eur. Soc. Photobiol. 1 (10), 834.

Canobbio, I., Guidetti, G.F., Oliviero, B., Manganaro, D., Vara, D., Torti, M., Pula, G., 2014. Amyloid β-peptide-dependent activation of human platelets: essential role for Ca2+ and ADP in aggregation and thrombus formation. Biochem. J. 462 (3), 513–523.

Casoli, T., Stefano, G.D., Giorgetti, B., Grossi, Y., Balietti, M., Fattoretti, P., Bertoni-Freddari, C., 2010. Release of β-amyloid from high-density platelets. Ann. N. Y. Acad. Sci. 1096 (1), 170–178.

Catricala, S., Torti, M., Ricevuti, G., 2012. Alzheimer disease and platelets: how's that relevant. Immun. Ageing 9 (1), 1–11.

Chen, M., Inestrosa, N.C., Ross, G.S., Fernandez, H.L., 1995. Platelets are the primary source of amyloid beta-peptide in human blood. Biochem. Biophys. Res. Commun. 213 (1), 96–103.

Diehl, B.G., Brown, N.R., 2014. Lignin cross-links with cysteine- and tyrosine-containing peptides under biomimetic conditions. J. Agric. Food Chem. 62 (42), 10312–10319.

Faccio, G., Kämpf, M.M., Piatti, C., Thöny-Meyer, L., Richter, M., 2014. Tyrosinase-catalyzed site-specific immobilization of engineered C-phycocyanin to surface. Sci. Rep. 4 (4), 5370.

Ferreira, S.T., Lourenco, M.V., Oliveira, M.M., De Felice, F.G., 2015. Soluble amyloid-beta oligomers as synaptotoxins leading to cognitive impairment in Alzheimer's disease. Front. Cell. Neurosci. 9.

Gao, Y., Cranston, R., 2010. Polytyrosine as an electroactive label for signal amplification in electrochemical immunosensors. Anal. Chim. Acta 659 (1-2), 109–114.

Gowert, N.S., Donner, L., Chatterjee, M., Eisele, Y.S., Towhid, S.T., Münzer, P., Walker, B., Ogorek, I., Borst, O., Grandoch, M., 2014. Blood platelets in the progression of Alzheimer's disease. PLoS One 9 (2) e90523.

Greenfield, N.J., 2006. Using circular dichroism spectra to estimate protein secondary structure. Nat. Protoc. 1 (6), 2876.
Hughes, J.C., Ingram, T.A., Jarvis, A., Denton, E., Lampshire, Z., Wernham, C., 2017. Consent for the diagnosis of preclinical dementia states: a review. Maturitas 98, 30–34.
Iqbal, K., Liu, F., Gong, C.-X., 2016. Tau and neurodegenerative disease: the story so far. Nat. Rev. Neurol. 12 (1), 15–27.
Janelidze, S., Stomrud, E., Palmqvist, S., Zetterberg, H., Van, W.D., Jeromin, A., Song, L., Hanlon, D., Tan, H.C., Baker, D., 2016. Plasma β-amyloid in Alzheimer's disease and vascular disease. Sci. Rep. 6, 26801.
Li, H., Huang, Y., Yu, Y., Li, G., Karamanos, Y., 2016. Self-catalyzed assembly of peptide scaffolded nanozyme as a dynamic biosensing system. ACS Appl. Mater. Interfaces 8 (4), 2833–2839.
Lowe, T.L., Strzelec, A., Kiessling, L.L., Murphy, R.M., 2001. Structure-function relationships for inhibitors of beta-amyloid toxicity containing the recognition sequence KLVFF. Biochemistry 40 (26), 7882–7889.
Mahmoud, S.F., Bialkowski, S.E., 1995. Detection of dityrosine in apoferritin. Appl. Spectrosc. 49 (11), 1677–1681.
Minamihata, K., Goto, M., Kamiya, N., 2011. Site-specific protein cross-linking by peroxidase-catalyzed activation of a tyrosine-containing peptide tag. Bioconjug. Chem. 22 (1), 74–81.
Mortamais, M., Ash, J.A., Harrison, J., Kaye, J., Kramer, J., Randolph, C., Pose, C., Albala, B., Ropacki, M., Ritchie, C.W., Ritchie, K., 2017. Detecting cognitive changes in preclinical Alzheimer's disease: a review of its feasibility. Alzheimer's Dementia 13 (4), 468–492.
Pérez-Grijalba, V., Pesini, P., Monleón, I., Boada, M., Tárraga, L., Ruiz-Laza, A., Martínez-Lage, P., San-José, I., Sarasa, M., 2013. Several direct and calculated biomarkers from the amyloid-β pool in blood are associated with an increased likelihood of suffering from mild cognitive impairment. Journal of Alzheimers Disease Jad 36 (1), 211–219.
Przedborski, S., 2017. The two-century journey of Parkinson disease research. Nat. Rev. Neurosci. 18 (4), 251–259.
Rissman, R.A., Trojanowski, J.Q., Shaw, L.M., Aisen, P.S., 2012. Longitudinal plasma amyloid beta as a biomarker of Alzheimer's disease. J. Neural Transm. 119 (7), 843–850.
Rosu, C., Cueto, R., Russo, P.S., 2016. Poly(colloid)s: “polymerization” of poly(l-tyrosine)-silica composite particles through the photoinduced cross-linking of unmodified proteins method. Langmuir. ACS. J. Surf. Colloids 32 (33), 8392.
Ruiz, A., Pesini, P., Espinosa, A., Perez-Grijalba, V., Valero, S., Sotolongo-Grau, O., Alegret, M., Monleon, I., Lafuentel, A., Buendia, M., Ibarria, M., Ruizl, S., Hernandez, I., San Jose, I., Tarraga, L., Boada, M., Sarasa, M., 2013. Blood amyloid beta levels in healthy, mild cognitive impairment and alzheimer's disease individuals: replication of diastolic blood pressure correlations and analysis of critical covariates. PLoS One 8 (11).
Saudou, F., Humbert, S., 2016. The biology of huntingtin. Neuron 89 (5), 910–926.
Schuster, J., Funke, S.A., 2016. Methods for the specific detection and quantitation of amyloid-beta oligomers in cerebrospinal fluid. J. Alzheimer's Dis. 53 (1), 53–67.
Sengupta, U., Nilson, A.N., Kayed, R., 2016. The role of amyloid-beta oligomers in toxicity, propagation, and immunotherapy. EBioMedicine 6, 42–49.
Shen, M.Y., Hsiao, G., Fong, T.H., Chen, H.M., Chou, D.S., Lin, C.H., Sheu, J.R., Hsu, C.Y., 2008. Amyloid beta peptide-activated signal pathways in human platelets. Eur. J. Pharmacol. 588 (2–3), 259–266.
Singleton, A., Hardy, J., 2016. The evolution of genetics: alzheimer's and Parkinson's diseases. Neuron 90 (6), 1154–1163.
Smirnov, A., Trupp, A., Henkel, A.W., Bloch, E., Reulbach, U., Lewczuk, P., Riggert, J., Kornhuber, J., Wiltfang, J., 2009. Differential processing and secretion of Abeta peptides and sAPPalpha in human platelets is regulated by thrombin and prostaglandine 2. Neurobiol. Aging 30 (10), 1552–1562.
Smith, L.M., Strittmatter, S.M., 2017. Binding sites for amyloid-beta oligomers and synaptic toxicity. Cold Spring Harb. Perspect. Med. 7 (5).
Song, F., Poljak, A., Valenzuela, M., Mayeux, R., Smythe, G.A., Sachdev, P.S., 2011. Meta-analysis of plasma amyloid-β levels in Alzheimer's disease. Journal of Alzheimers Disease Jad 26 (26), 365–375.
Takahashi, R.H., Nagao, T., Gouras, G.K., 2017. Plaque formation and the intraneuronal accumulation of beta-amyloid in Alzheimer's disease. Pathol. Int. 67 (4), 185–193.
Toledo, J.B., Shaw, L.M., Trojanowski, J.Q., 2013. Plasma amyloid beta measurements - a desired but elusive Alzheimer's disease biomarker. Alzheimer's Res. Ther. 5 (2).
Viola, K.L., Klein, W.L., 2015. Amyloid beta oligomers in Alzheimer's disease pathogenesis, treatment, and diagnosis. Acta Neuropathol. 129 (2), 183–206.
Wang, Y., Boysen, R.I., Wood, B.R., Kansiz, M., Mcnaughton, D., Hearn, M.T., 2008. Determination of the secondary structure of proteins in different environments by FTIR-ATR spectroscopy and PLS regression. Biopolymers 89 (11), 895.
Widrig, C.A., Chung, C., Porter, M.D., 1991. The electrochemical desorption of n-alkanethiol monolayers from polycrystalline Au and Ag electrodes. J. Electroanal. Chem. 310 (1-2), 335–359.
Xue, C., Lin, T.Y., Chang, D., Guo, Z., 2017. Thioflavin T as an amyloid dye: fibril quantification, optimal concentration and effect on aggregation. R. Soc. Open. Sci. 4 (1), 160696.